Available online at www.sciencedirect.com
SCIENCE DIRECT
Biochimica et Biophysica Acta 1758 (2006) 627–635
BIOCHIMICA ET BIOPHYSICA ACTA
BBA
http://www.elsevier.com/locate/bba

# Functional involvement of membrane-embedded and conserved acidic residues in the ShaA subunit of the multigene-encoded $Na^+/H^+$ antiporter in *Bacillus subtilis*

Saori Kosono [a,*], Yusuke Kajiyama [a,b], Shin Kawasaki [a], Toko Yoshinaka [a], Koki Haga [a], Toshiaki Kudo [a,c]

[a] *Environmental Molecular Biology Laboratory, RIKEN, Wako, Saitama 351-0198, Japan*
[b] *Department of Applied Biology, Faculty of Textile Science and Technology, Shinshu University, Ueda, Nagano 386-8567, Japan*
[c] *Graduate School of Integrated Science, Yokohama City University, Tsurumi, Kanagawa 230-0045, Japan*

Received 26 October 2005; received in revised form 23 February 2006; accepted 4 April 2006
Available online 26 April 2006

**Abstract**

ShaA, a member of a multigene-encoded $Na^+/H^+$ antiporter in *B. subtilis*, is a large integral membrane protein consisting of 20 transmembrane helices (TM). Conservation of ShaA-like protein subunits in several cation-coupled enzymes, including the NuoL (ND5) subunit of the $H^+$-translocating complex I, suggests the involvement of ShaA in cation transport. *Bacillus subtilis* ShaA contains six acidic residues that are conserved in ShaA homologues and are located in putative transmembrane helices. We examined the functional involvement of the six transmembrane acidic residues of ShaA by site-directed mutagenesis. Mutation in glutamate (Glu)-113 in TM-4, Glu-657 in TM-18, aspartate (Asp)-734 and Glu-747 in TM-20 abolished the antiport activity, suggesting that these residues play important roles in the ion transport of Sha. The acidic group was necessary and sufficient in Glu-657 and Asp-743, while it was not true of Glu-113 and Glu-747. Mutation in Asp-103 in TM-3, which is conserved in ShaA-types but not in ShaAB-types, partially affected on the antiport activity. Mutation in Asp-50 in TM-2 resulted in a unexpected phenotype: mutants retained the wild type level of ability to confer NaCl resistance to the $Na^+/H^+$ antiporter-deficient *E. coli* KNabc, but showed a very low antiport activity. The acidic group of Asp-50 and Asp-103 was not essential for the function. Our results suggested that these acidic residues are functionally involved in the ion transport of Sha, and some of them probably in cation binding and/or translocation.


*Keywords:* A multigene-encoded $Na^+/H^+$ antiporter; NuoL; Transmembrane topology; Conserved acidic residues; Site-directed mutagenesis:*Bacillus subtilis*

## 1. Introduction

Sha (sodium hydrogen antiporter, also known as Mrp [1], Mnh [2] or Pha [3]) is a monovalent cation/proton antiporter encoded by conserved six- or seven-gene clusters that are conserved among the genomes of bacteria and archaea (recently reviewed in [4]). Mutations in *sha* homologues result in marked pH or salt-sensitive phenotypes that are not observed with other antiporters. Thus, the Sha antiporter is likely critical for the homeostasis of cytoplasmic pH and monovalent cations [1,3,5–7]. The substantial homeostatic capacity of the Sha antiporter is correlated with a putative multi-subunit complex structure, which is comprised of large A, D subunits and small B, C, E, F and G subunits. In the six gene-membered types, subunits A and B are fused into one AB subunit [4,8]. All of the Sha subunits appear to be necessary for the transport function because deletions of any one of Sha subunits results in the loss or impairment of function [2,3,9,10]. Despite the progress in characterization of Sha subunits, there is still little known about the molecular structure of the putative multisubunit complex or the role that each subunit plays in the transport function.

Primary sequence relationships between Sha proteins and subunits of $H^+$-translocating NADH: quinone oxidoreductase (complex I) have been of interest ever since the Sha antiporter was first identified in the alkaliphilic *Bacillus halodurans* C-125 [5]. A recent bioinformatics-based study by Mathiesen and Hägerhäll demonstrated that ShaA, ShaC and ShaD are evolutionally related

* Corresponding author. Tel.: +81 48 467 9545; fax: +81 48 462 4672.
*E-mail address:* kosono@riken.jp (S. Kosono).

0005-2736/$ - see front matter © 2006 Elsevier B.V. All rights reserved.
doi:10.1016/j.bbamem.2006.04.012

to NuoL, NuoK, and NuoM/N of the bacterial complex I, respectively [8]. Like the NuoL, M and N subunits, ShaA and D proteins are homologous to each other. Although the roles of NuoL, M and N subunits in the bacterial complex I are not exactly clear, these subunits have been implicated in proton translocation based on their location in the membrane and their primary sequence similarity to Sha antiporter proteins [11–13]. ShaA/D-like protein subunits are also found in Mbh in *Pyrococcus furiosus*, which is a membrane-bound hydrogenase that is involved in the $H^+$-coupled $H_2$-production during the generation of a proton motive force [14–16]. The conservation of ShaA/D-like protein subunits in these $H^+$ and/or $Na^+$-translocating enzymes would support the idea that these subunits are involved in cation translocation. However, there is currently no evidence for any cation translocation site(s) in the Sha antiporter or the direct involvement of subunits A and/or D in cation translocation.

In many cation-coupled transporters, it has been well documented that negatively charged residues in transmembrane helices are important for cation binding and/or translocation [17]. Recently, it has been reported that the membranous Nuo subunits contain membrane-embedded acidic residues involved in the function of the complex I [18,19]. Here, we use site-directed mutagenesis to address the functional involvement of conserved acidic residues (Asp and Glu) in the transmembrane helices of the ShaA protein.

## 2. Materials and methods

### 2.1. Construction of B. subtilis sha-expressing plasmids

To clone the *sha*/*mrp* cluster of *B. subtilis*, the cluster was PCR-amplified in two fragments (*sha*-front and *sha*-back), using primers shaSD-F and Bbm-R, and Bbm-F and Gpst-R, respectively, shown in Table 1. The *Bam*HI site was introduced at the 3' and 5′ ends of the *sha*-front and *sha*-back, respectively, to connect the two fragments without changing the Gly-88 residue in the *shaB*-coding region. A ribosome-binding site (AGGA) was introduced upstream of the *shaA* start codon. The two amplified fragments were ligated in the low-copy number *E. coli* vector pTWV228 (Takara), resulting in the plasmid pTY11, which expresses the *sha*/*mrp* cluster under the *lac*Z promoter. To construct pKS19 to 24 (Ala-replacements) and pKY19 to 32 (other replacements), the *sha*-front region was amplified in two sub-fragments using the primers listed in Table 1. During PCR amplifications, site-directed mutations were introduced to change a target acidic residue into non-charged alanine, aspartate or glutamate, or asparagine or glutamine, and the two sub-fragments were connected by ligation. All mutations and connection sites were verified by DNA sequencing. The *sha*-front of pTY11 was replaced with the corresponding fragments containing a site-directed mutation in *shaA*, resulting the plasmids listed in Table 2.

### 2.2. Growth conditions

*E. coli* KNabc (Δ*nhaA*::$Km^R$, Δ*nhaB*::$Em^R$, Δ*chaA*::$Cm^R$) [20] cells containing *sha*-expressing plasmids were routinely cultivated at 37 °C in the LBK medium containing 10 g/l tryptone, 5 g/l yeast extract, 10 g/l KCl, 1 mM IPTG, 100 μg/ml ampicillin, 30 μg/ml kanamycin, 30 μg/ml chloramphenicol, and 160 μg/ml erythromycin. For assays of NaCl resistance during growth, concentrations of NaCl were added to the LBK medium as indicated.

### 2.3. $Na^+/H^+$ antiport activity

Activity of $Na^+/H^+$ antiporter was measured by a quenching method with everted membrane vesicles, as described previously [7,21]. KNabc cells were grown at 37 °C in LBK medium to the late exponential phase of growth (1.0–1.3 in $OD_{600}$), and everted membrane vesicles were prepared in TSCD buffer (10 mM Tris–HCl pH 7.5, 140 mM choline chloride, 0.25 M sucrose and 0.5 mM DTT). The reaction mixture (2 ml) contained 50 mM bis–tris propane, 140 mM KCl, and 5 mM $MgCl_2$, and was adjusted to the indicated pH. After the addition of acridine orange (2 μM) and membrane vesicles (50 μg of protein measured by the *RC DC* protein assay kit (Bio-Rad)), 10 mM tris-lactate was added to generate a ΔpH, which was accompanied by quenching of the fluorescence. Fluorescence of acridine orange was monitored with excitation at 493 nm and emission at 530 nm.

Table 1
Primers used for construction of the site-directed mutations in this study

| Primers | DNA sequence |
|---|---|
| shaSD-F | 5′-cgg GA ATT CAG GAT ACT AGT ATG CAT ACG GGC TGG TTT G-3′ |
| Bbm-F | 5′-cg GGa TCC TTT GTC TTC GGG GCT CC-3′ |
| Bbm-R | 5′-cg GGA tCC AAC GCC TGT TAA TAC AGC-3 |
| Gpst-R | 5′-tgca CTG CAG TTA TAA ATA AGA ATC CTC-3′ |
| D50A-F | 5′-cag a GGC CTC GGG TTA TTA TTC GCT TTA C-3′ |
| D50A-R | 5′-cgc AG GCC *tgC* TAT ATA AAC GGT AAA G-3′ |
| D50E-F | 5′-*GAa* GGC CTC GGG TTA TTA TTC-3′ |
| D50N-F | 5′-*aAC* GGC CTC GGG TTA TTA TTC-3′ |
| D50-R | 5′-TAT ATA AAC GGT AAA GTT AAT-3′ |
| D103A-F | 5′-gac Tg *GcC* AAT GTC ATG GTT CTC TAC ATG-3′ |
| D103A-R | 5′-tat T *GgC* cAC TAG AAC GAC GCC GAG CAT G-3′ |
| D103E-F | 5′-*GAa* AAT GTC ATG GTT CTC TAC-3′ |
| D103N-F | 5′-*aAC* AAT GTC ATG GTT CTC TAC-3′ |
| D103-R | 5′-AAA TCC CCT GAA ATC AAC GAG-3′ |
| E113A-F | 5′-cgc G tta ACA AGC CTT TCA TCC TTT TTG C-3′ |
| E113A-R | 5′-gct GT taa *CgC* CCA GAA CAT GTA GAG AAC C-3′ |
| E113D-F | 5′-*GAc* CTT ACA AGC CTT TCA TCC-3′ |
| E113Q-F | 5′-*cAG* CTT ACA AGC CTT TCA TCC-3′ |
| E113-R | 5′-CCA GAA CAT GTA GAG AAC CAT-3′ |
| E657A-F | 5′-tca Tc *Gcg* ACG ATT TCT GTG GCA CTG TTT C-3′ |
| E657A-R | 5′-tag T *cgC* gAT GAC GAG CTG AGT CAA TGC C-3′ |
| E657D-F | 5′-*GAa* ACG ATT TCT GTG GCA CTG-3′ |
| E657Q-F | 5′-*cAA* ACG ATT TCT GTG GCA CTG-3′ |
| E657-R | 5′-AAT GAC GAG CTG AGT CAA TGC-3′ |
| D743A-F | 5′-*GcT* ACA ATG TTT GAA ATT ACG-3′ |
| D743E-F | 5′-*GAa* ACA ATG TTT GAA ATT ACG-3′ |
| D743N-F | 5′-*aAT* ACA ATG TTT GAA ATT ACG-3′ |
| D743-R | 5′-AAA TCC CCT GAA ATC AAC GAG-3′ |
| E747A-F | 5′-*GcA* ATT ACG GTA TTA ACG ATA-3′ |
| E747D-F | 5′-*GAt* ATT ACG GTA TTA ACG ATA-3′ |
| E747Q-F | 5′-*cAA* ATT ACG GTA TTA ACG ATA-3′ |
| E747-R | 5′-AAA CAT TGT ATC AAA TCC CCT-3′ |

Restriction sites and the start codon of *shaA* are underlined.
Codons substituted are shown in italic.
Mismatch bases are shown by small letters.

### 2.4. Multiple alignment and prediction of transmembrane topology

Multiple alignment of the primary sequences was performed by ClustalX [22] using default parameters. Available amino acid sequences of ShaA and NuoL homologues were retrieved from NCBI, TIGR, or SwissProt databases, and the accession numbers are shown in the legend of Fig. 1. Prediction of the transmembrane topology was carried out by six methods: SOSUI [23], TMHMM [24], HMMTOP [25], TMPred [26], PHDhtm [27] and DAS [28]. All methods were used with their default values. The TMHMM, HMMTOP and TMPred methods were also used to predict the orientation of the protein in the membrane.

### 2.5. Western blot

Western blot analysis was carried out to confirm the expression of *sha* gene products. Membrane vesicles that were prepared in Section 2.3 were suspended in SDS-sample buffer (50 mM Tris–HCl pH 6.8, 0.2% SDS, 6% β-mercaptoethanol

Table 2
Growth and antiport activity of mutants in transmembrane conserved acidic residues

| Plasmid | Mutation | Growth[a] at indicated NaCl concentration of | | | | Antiport activity[b] | | | |
|---|---|---|---|---|---|---|---|---|---|
| | | 0 M | 0.2 M | 0.4 M | 0.6 M | pH 6.5 | pH 7.5 | pH 8.0 | pH 8.5 |
| pTY11 | WT | 3.06±0.14 | 2.29±0.25 | 1.23±0.15 | 0.44±0.11 | NA | 3.6±0.9 | 5.0±1.5 | 6.0±1.8 |
| pTWV228 | NC | 3.40±0.09 | 0.27±0.16 | 0.03±0.02 | 0.02±0.01 | NA | 1.2±1.3 | 0.7±0.9 | 1.8±2.1 |
| pKS19 | D50A | 3.14±0.20 | **2.48±0.12** | **1.27±0.19** | **0.32±0.08** | NA | 2.2±0.7 | 0.0±0.2 | 1.7±0.5 |
| pKY19 | D50E | 3.28±0.06 | **2.44±0.21** | **1.16±0.21** | **0.35±0.12** | NA | 1.4±0.7 | 2.9±1.2 | 2.7±0.2 |
| pKY20 | D50N | 3.20±0.22 | **2.57±0.06** | **1.74±0.22** | **0.60±0.07** | NA | 2.3±0.7 | 2.7±0.5 | 2.3±1.0 |
| pKS20 | D103A | 3.36±0.12 | **1.17±0.11** | 0.10±0.04 | 0.01±0.00 | NA | 2.1±0.4 | 1.0±0.6 | 3.4±0.4 |
| pKY21 | D103E | 3.33±0.09 | **1.07±0.49** | 0.10±0.08 | 0.01±0.00 | NA | 2.5±0.6 | **3.2±0.3** | −2.0±0.8 |
| pKY22 | D103N | 3.19±0.29 | **2.00±0.19** | **0.83±0.38** | 0.04±0.03 | NA | **4.6±0.6** | **4.2±0.5** | **4.4±0.2** |
| pKS21 | E113A | 3.26±0.03 | 0.03±0.00 | 0.01±0.00 | 0.01±0.00 | NA | 0.9±0.3 | −0.4±0.9 | 2.3±0.9 |
| pKY23 | E113D | 3.05±0.14 | **1.86±0.23** | **0.46±0.17** | 0.05±0.02 | NA | 1.9±0.6 | 1.4±0.9 | 3.7±2.0 |
| pKY24 | E113Q | 3.40±0.11 | 0.01±0.00 | 0.01±0.00 | 0.01±0.00 | NA | 1.5±0.4 | 0.8±0.3 | 1.3±1.9 |
| pKS22 | E657A | 3.32±0.09 | 0.20±0.07 | 0.01±0.00 | 0.01±0.00 | NA | 0.5±0.2 | 1.3±0.5 | 1.5±0.9 |
| pKY25 | E657D | 3.10±0.12 | **2.20±0.12** | **1.19±0.09** | **0.47±0.14** | NA | **3.3±0.5** | **4.9±0.6** | **5.7±0.7** |
| pKY26 | E657Q | 3.15±0.01 | 0.46±0.08 | 0.14±0.01 | 0.04±0.00 | NA | 1.0±0.5 | −0.3±0.7 | 1.9±0.5 |
| pKY27 | D743A | 3.42±0.02 | 0.08±0.03 | 0.01±0.01 | 0.01±0.00 | NA | 0.4±0.2 | 0.3±0.4 | 0.3±0.4 |
| pKY28 | D743E | 3.21±0.11 | **2.42±0.06** | **1.31±0.07** | **0.40±0.13** | NA | **3.6±0.3** | **8.5±0.2** | **7.9±0.5** |
| pKY29 | D743N | 2.97±0.22 | 0.22±0.07 | 0.01±0.01 | 0.01±0.01 | NA | 1.1±0.3 | 1.1±0.1 | 0.6±0.3 |
| pKY30 | E747A | 3.09±0.10 | 0.03±0.02 | 0.03±0.03 | 0.01±0.00 | NA | 0.6±0.4 | 0.4±1.3 | 1.4±2.2 |
| pKY31 | E747D | 3.18±0.20 | **2.12±0.24** | **0.41±0.15** | 0.06±0.02 | NA | 0.5±0.2 | 1.5±0.4 | 1.6±0.8 |
| pKY32 | E747Q | 3.10±0.04 | 0.05±0.01 | 0.01±0.00 | 0.01±0.00 | NA | 0.9±0.2 | 0.9±0.4 | 1.8±1.7 |

Values of mutants that significantly exceed those of NC in the same conditions are shown in bold.
WT, wild type; NC, negative control; NA, no activity.
[a] KNabc cells were grown in LBK medium containing indicated concentrations of NaCl and the growth was evaluated by $OD_{600}$ after 8 h of inoculation. Values are shown as the means and standard deviations of two experiments with duplicates.
[b] The antiport activity is shown as the percentage fluorescence dequenching upon addition of 10 mM NaCl, from which the percentage dequenching without addition of NaCl is subtracted. Values are shown as the means and standard deviations of more than three replicates.

and 10% glycerol), and 15 micrograms of protein was loaded onto a 6–20% gradient SDS-polyacrylamide gel without boiling. A polyclonal anti-ShaE antibody, prepared from a rabbit immunized with purified histidine (His)-tagged *B. subtilis* ShaE proteins, was used at a 1:2000 dilution.

## 3. Results

### *3.1. Identification of putatively transmembrane conserved acidic residues of ShaA protein*

Multiple alignments of the primary sequences of ShaA, ShaAB and NuoL homologues were performed using ClustalX with default settings. Then, prediction of their transmembrane topology were carried out by six methods: SOSUI, TMHMM, HMM TOP, TMPred, PHDhtm and DAS. All methods were used with their default values. Consistent with the previous report of Mathiesen and Hägerhäll [13], *B. subtilis* ShaA protein was predicted to have 20 transmembrane segments (TM) (19 strongly and 1 weakly agreed upon), with the N and C termini oriented in the cytoplasm (Figs. 1 and 2). A few methods (TMHMM, HMM TOP, and PHDhtm) weakly agreed upon a prediction for TM-7, but this putative transmembrane segment overlapped with the highly conserved region in the corresponding 196 to 229 positions of *B. subtilis* ShaA (Fig. 1). A possible quinone-binding motif (L/A/V-$X_3$-H-$X_2$-T/N) is found in the TM-10 [29,30]. The corresponding TMs-9 and 10 of *R. capsulatus* NuoL are reported to be located on the inside of the membrane surface [13]. The N-terminal regions in *B. subtilis* ShaA containing TMs-1 to 13 share similarity in sequence and topology to NuoL homologues.

Twelve acidic residues were found to be conserved among ShaA/AB homologues. That is, Asp-50, Glu-113, Asp-270, Asp-334, Asp-341, Glu-379, Glu-441, Asp-648, Glu-657, Asp-738, Asp-743, and Glu-747 were present in the corresponding positions of *B. subtilis* ShaA (Fig. 1). The Asp-50, Glu-113 and Asp-270 residues were also conserved in NuoL homologues. Of the above 12 conserved acidic residues, Asp-50 in TM-2 (SOSUI, TMPred, PHDhtm and DAS agreed), Glu-113 in TM-4 (all except DAS agreed), Glu-657 in TM-18 (all methods agreed), Asp-743 in TM-20 (SOSUI agreed) and Glu-747 in TM-20 (SOSUI, TMHMM, HMMTOP and TMPred agreed) were predicted to be located in the transmembrane segments (Figs. 1 and 2). In addition to the above five acidic residues, the Asp 103 residue in TM-3 (SOSUI, TMPred, PHDhtm and DAS agreed) was chosen for further analysis because it is well conserved in ShaA and NuoL homologues, but not in ShaAB homologues, and because it is putatively located within a transmembrane segment.

### *3.2. The effect of site-directed mutations in transmembrane conserved acidic residues on the growth phenotype*

We used site-directed mutagenesis to change each Asp-50, Asp-103, Glu-113, Glu-657, Asp-743, and Glu-747 residue to another acidic residue (Glu to Asp or Asp to Glu), the amido residue (Glu to Gln or Asp to Asn), or non-charged residue alanine, then we examined the effects of these mutations on the Sha function. The plasmid pTY11 was used to express the wild-type *sha*/*mrpABCDEFG* cluster under control of the *lac* promoter.


Fig. 1. Alignment and transmembrane topology of ShaA/AB and NuoL homologues from six selected species: *B. subtilis* Sha/MrpA (BsuShaA, Q9K2S2), *Staphylococcus aureus* MnhA (SauMnhA, P60675), *Pseudomonas aeruginosa* PA1054 (PaeShaAB, AAG04443), S. *meliloti* PhaAB (SmePhaAB, Q52978), *E. coli* NuoL (EcoNuoL, P33607), *Rhodobacter capsulatus* NuoL (RcaNuoL, P50939). Amino acid residues conserved in all sequences are marked by asterisks. Acidic residues conserved in ShaA/AB homologues are shown by exclamation marks. The six acidic residues characterized in this study are shown in red. The stretches of residues in which four or more of six methods agreed in their prediction of a transmembrane segment are highlighted in yellow, and areas in which three or fewer methods agreed are in cyan. The predicted orientation of the transmembrane segments is shown with i (=inside) and o (=outside), based on the analysis of *B. subtilis* ShaA by the HMMTOP method only. TMHMM also gave a similar result of the orientation, but TMPred did not. A possible Q-binding motif (L/A/V-$X_3$-H-$X_2$-T/N) [29,30] in TM 10 is indicated by a boxed line. A highly conserved region among ShaA/AB and NuoL homologues is indicated by a dot-boxed line.

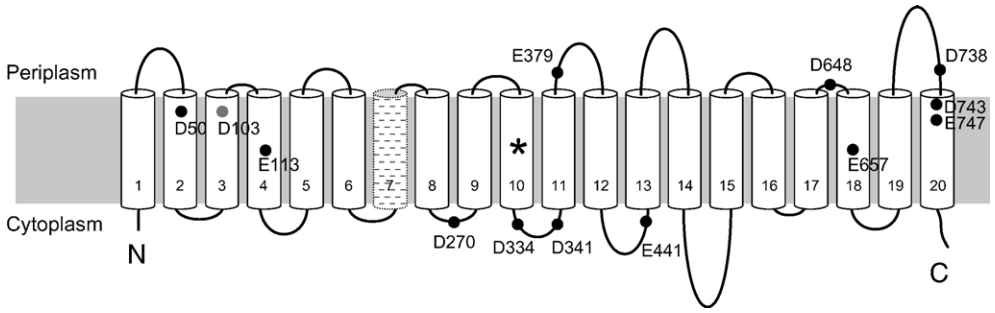


Fig. 2. Transmembrane topology model of ShaA protein of *B. subtilis*. Positions of twelve acidic residues conserved in ShaA/AB homologues and D103 residue conserved in ShaA homologues are shown by black and gray dots, respectively. TM-7, which is weakly agreed upon in its prediction, is shown by a hatched-lined column. A Q-binding motif in TM10 is indicated by an asterisk.

We also constructed eighteen plasmids to express a *sha* cluster containing a site-directed mutation in *shaA* (listed in Table 2). These plasmids were introduced into the $Na^+/H^+$ antiporter-deficient *E. coli* KNabc [20], which shows severely inhibited growth in/on NaCl, and undetectable $Na^+/H^+$ antiport activity.

To estimate the $Na^+/H^+$ antiport activity of cells harboring the *sha*-expressing plasmid derivatives, we first examined restoration of the growth defect of KNabc cells in LBK medium containing various concentrations of NaCl. The growth curves of KNabc cells with the plasmid pTY11 (containing the wild type *sha*) and pTWV228 (the negative control) were shown in Fig. 3. pTY11 restored the growth defect of KNabc in the presence of up to 0.6 M NaCl. The growth of KNabc in/on 0.2 M NaCl is conventionally used to judge whether the introduced plasmid is responsible for $Na^+/H^+$ antiporter activity or not [2,20]. In our culture conditions, however, KNabc cells with pTWV228 sometimes showed a weak growth in the presence of 0.2 M NaCl. We evaluated the growth capacity of mutant plasmids by $OD_{600}$ after 8 h of cultivation, at the timing when KNabc with pTY11 reached to the stationary phase of growth in the presence of 0.2 M NaCl. As summarized in Table 2, in the absence of added NaCl, no difference was observed in the growth among the wild type, negative control and mutant derivatives. pKS19 (D50A), pKY19 (D50E), pKY20 (D50N), pKY23 (E657D) and pKY28 (D743E) conferred NaCl resistance in the growth in the presence of 0.6 M NaCl, similar to the level of the wild type. In contrast, pKS21 (E113A), pKY24 (E113Q), pKS22 (E657A), pKY27 (D743A), pKY29 (D743N), pKY30 (E747A) and pKY32 (E747Q) showed NaCl sensitivity similar to that of the negative control. Other mutant plasmids (pKS20 (D103A), pKY21 (D103E), pKY22 (D103N), pKY23 (E113D), pKY26 (E657Q) and pKY31 (E747D) conferred partial restoration in the growth defect. The growth phenotypes were also confirmed on LBK agar plates, which gave similar patterns to the growth phenotypes in liquid cultivation (data not shown).

From Table 2, mutations in the D50 residue appeared not to affect substantially on the function of ShaA. Since the D50 mutants conferred NaCl resistance similar to that of the wild type regardless of the acidic group, the acidic group of this residue was not essential for the ion transport of ShaA. In contrast, in the case of the E657 and D743 residues, mutations that retain the acidic group had no effect on the growth capacity, but mutations that lose the acidic group abolished the capacity,

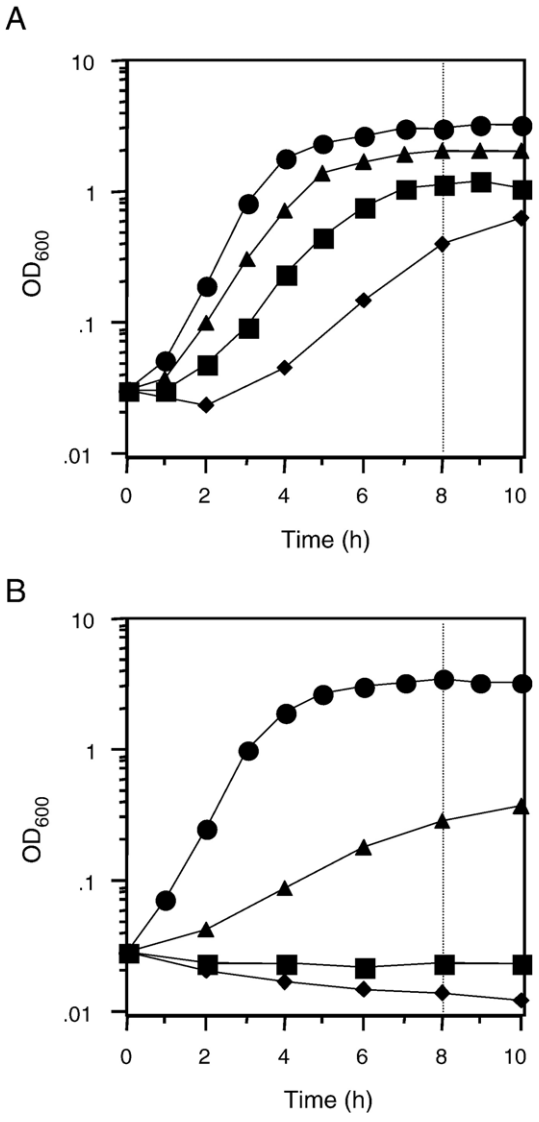


Fig. 3. Growth curves of *E. coli* KNabc cells complemented by *sha*-expressing plasmids. KNabc cells containing pTY11 (the wild type *sha*) (A) or pTWV228 (the negative control) (B) were grown in LBK medium containing ampicillin, IPTG and 0 M (circle), 0.2 M (triangle), 0.4 M (square) or 0.6 M (diamond) of NaCl. The growth capacity of mutant plasmids was evaluated by $OD_{600}$ after 8 h of cultivation, shown in Table 2.

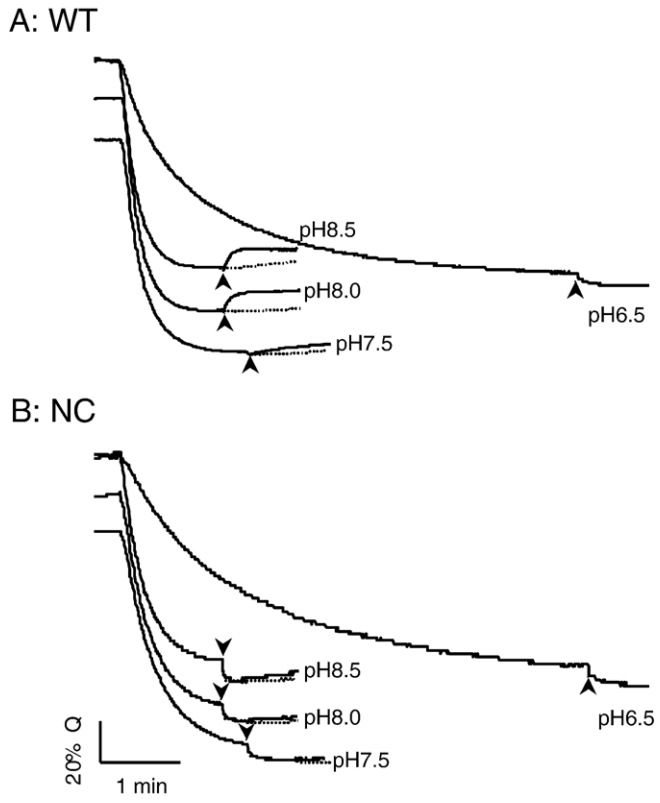


Fig. 4. $Na^+/H^+$ antiport activity of the *B. subtilis* Sha antiporter in everted membrane vesicles. Everted membrane vesicles were prepared from KNabc cells containing pTY11 (the wild type *sha*) (A) or pTWV228 (the negative control) (B). Assays were performed in a mixture (2 ml) containing 50 mM bis–tris propane, 140 mM KCl, 5 mM $MgCl_2$, 2 μM acridine orange and membrane vesicles (50 μg of protein). Fluorescence quenching was initiated by addition of 2 mM Tris–lactate and was recorded until it reached at a steady state. Then, 10 mM NaCl was added at the timing indicated by arrows to elicit $Na^+/H^+$ antiport activity. Fluorescence curves without addition of NaCl are shown by hatched lines.

suggesting that the acidic group was important in these residues. In the case of E113 and E747, the mutants that retain the acidic group conferred NaCl resistance higher than the other mutants, but did not reach to the wild type level, suggesting that other factors besides the acidic group were also important and thus these residues seemed to play a critical role in the ion transport. In the case of the D103 residue, the D103N mutant conferred NaCl resistance higher than the other variants, suggesting that the acidic group was not likely important, similar to the case of the D50 residue.

### *3.3. The effect of site-directed mutations on the $Na^+/H^+$ antiport activity*

We next used a fluorescence quenching method to examine $Na^+/H^+$ antiport activity in everted membrane vesicles of KN abc strains. As previously reported [2,7,31], the $Na^+/H^+$ antiport activity (the percentage fluorescence dequenching upon addition of NaCl) of the Sha/Mrp antiporter was relatively low compared to those of NhaA or other antiporters. In our assay conditions, a slight recovery of fluorescence quenching was observed without addition of NaCl or in the negative control (Fig. 4), which interfered evaluation of the Sha-dependent activity. We thus calculated the antiport activity by subtracting the % dequenching without addition of NaCl from that upon addition of NaCl. The $Na^+/H^+$ antiport activity of the wild type Sha showed pH dependence with a pH profile similar to NhaA of *E. coli* [32] and Sha of *P. aeruginosa* [7]. That is, the activity was higher at pH 8.5 (6.0±1.8%) and pH 8.0 (5.0±1.5%) than at pH 7.5 (3.6±0.9%), and barely detectable at pH 6.5 (Table 2 and Fig. 4A).

The mutants E657D and D743E, which conferred NaCl resistance in the growth identical to that of the wild type, showed equivalent (E657D) or slightly higher (D743E) levels of the antiport activity compared to the wild type at pH 7.5 to 8.5 (Table 2 and Fig. 5C and D). Unexpectedly, all D50 mutants that conferred NaCl resistance as high as the wild type showed a low or undetectable activity (Table 2 and Fig. 5A). The D103N mutant, which conferred partial restoration in the growth defect of KNabc, showed a substantial activity (Table 2 and Fig. 5B). We could not detect the activity significantly different from the negative control with the other mutants that showed negative as well as partial phenotypes in the growth, except the case of the D103E mutant at pH 8.0 (Table 2).

Due to the very low activity, it was difficult to determine accurately the pH profile of the mutants. However, it appeared

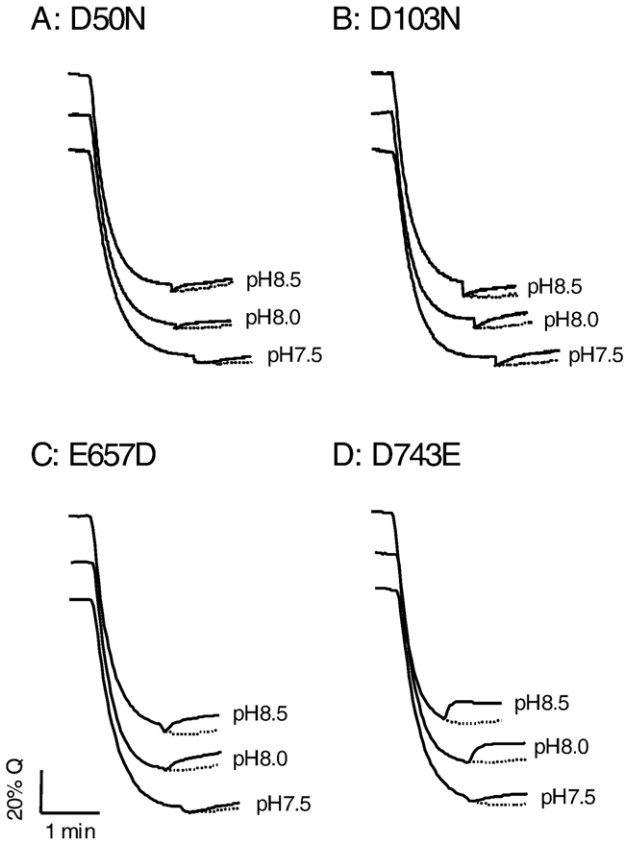


Fig. 5. $Na^+/H^+$ antiport activity of the selected mutants. (A) the D50N mutant, (B) the D103N mutant, (C) the E657D mutant and (D) the D743E mutant. Methods are described in the legend of Fig. 4.

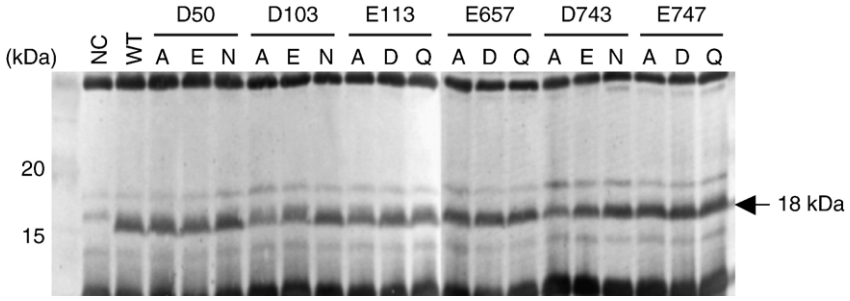


Fig. 6. Western blot of membrane proteins from *E. coli* KNabc cells. 15 μg of total membrane protein from each strain was loaded onto a 6–20% gradient DS-polyacrylamide gel, then blotted onto a PVDF membrane. ShaE proteins were detected by probing with an anti-ShaE antibody from rabbit. Membrane proteins of pTWV228-transformed KNabc cells were used as a negative control (NC). Precision plus protein standards (Bio-Rad) were used as a molecular weight marker (on the left).

that E657D and D743E retained the pH dependence of Sha and the activity of D103N seemed to be constitutive at pH 7.5 to 8.5 (Table 2 and Fig. 5).

We used western blot analysis to determine if the differences in the growth phenotype and $Na^+/H^+$ antiport activity observed with the mutant plasmids were caused by strain-dependent variations in protein expression. The levels of ShaE proteins in the membrane were approximately equivalent among the derivatives (Fig. 6), suggesting that at least the translation of *sha* mRNA and the sorting of Sha proteins to the membrane was normal. Although we unfortunately did not detect ShaA protein itself, our western blot results suggest that the growth phenotypes and antiport activities of strains that harbored mutant plasmids likely resulted from the properties of the mutations rather than from difference in the expression levels of Sha proteins. We cannot exclude a possibility that the mutations might affect functional assembly and/or interactions of Sha proteins in the putative complex.

## 4. Discussion

We identified transmembrane conserved acidic residues in ShaA that are functionally important for the Sha antiporter. Mutations in Glu-113, Glu-657, Asp-743 and Glu-747 abolished the growth capacity and antiport activity, indicating that these residues make large contributions to the ion transport of Sha. The acidic group was necessary and sufficient in Glu-657 and Asp-743. In contrast, Glu-113 and Glu-747 seemed to be more essential, because the Asp-replacements conferred only a partial restoration in the growth defect. Though the structural information of the Sha antiporter is not available, we speculate that some of these residues may be involved in cation binding and/or translocation in the Sha antiporter. The Glu-113 residue is especially interesting because it is positioned in the middle of the membrane and highly conserved not only in ShaA/AB and NuoL homologues, but also in ShaD, NuoM and N homologues. Steuber made an interesting report that a C-terminally truncated NuoL that contains the corresponding Glu-113 residue (Glu-144 in NuoL of *E. coli*) is responsible for $Na^+$ permeability [33]. Although the Glu-144 residue in NuoL remains to be characterized, our results suggest that it is likely to be important for the function of the complex I.

Mutants of the Asp-50 residues are puzzling. They conferred NaCl resistance as high as the wild type, but showed a very low or undetectable antiport activity. We confirmed the result certainly. We do not have at present any suitable explanation for the gap between the growth and transport phenotypes. We found similar phenotypes in some mutants (A127C/G338C, P129C/G338C and A137C/G338C) of *E. coli* NhaA, which conferred NaCl resistance identical to that of the wild type on 0.6 M NaCl, but showed less than 10% antiport activity of the wild type [34]. We could imagine a possibility that such low activity is sufficient to support the growth on 0.6 M NaCl. Alternatively, in the case of the Sha antiporter that is expected to have a primary energization mode of transport [31,35], it could be imagined that $H^+$-uncoupled $Na^+$ transport might exist and support NaCl resistance in the growth. From our preliminary results, the antiport activity of the Asp-50 mutants was not recovered upon addition of high concentration of NaCl (100 mM), suggesting that these mutants were not affected only in the apparent Km [34]. We will need to determine in more detail ion transport properties of the Asp-50 mutants in other assay conditions or methods to find a reason for the unexpected result. Since Asp-50 is well conserved in not only ShaA/AB but also NuoL homologues, the corresponding Asp-50 residue might also have a role in the function of the complex I. Many single gene-type $Na^+/H^+$ antiporters also conserve an Asp residue in an N-terminal transmembrane segment, as described by Dibrov and Fliegel [17]. NhaA of *E. coli* contains such an Asp residue (Asp-65), but it has been shown to be dispensable for both growth capacity and antiport activity [36]. Thus, our result indicates that the Asp-50 residue of *B. subtilis* ShaA behaves differently from Asp-65 of *E. coli* NhaA.

The Asp-103 residue is also considered to be involved in the ion transport of Sha, since mutations in this residue affected the growth and transport activities. The size of the side chain rather than the acidic group seems to be important. The corresponding residue is not conserved among ShaAB homologues (Glu in *P. aeruginosa* ShaAB and Gly in *S. meliloti* PhaAB), supporting the idea that the acidic group is not essential in this residue. The importance of the size of the side chain may suggest that the spatial position of the residue in the molecular architecture of Sha is important.

Recently, the crystal structure of NhaA, the main $Na^+/H^+$ antiporter of *E. coli*, has been solved, and several important

roles of acidic residues have been revealed [37]. Asp-163 and Asp-164 of helix V, which reside in the middle of the membrane and are highly conserved and essential, are proposed to be the putative $Na^+/Li^+$-binding site of NhaA. Glu-113, Glu-657 and Glu-747 of *B. subtilis* ShaA are similar to Asp-163 and Asp-164 of *E. coli* NhaA in terms of their essentiality in transport, their location in the middle of membrane, and their high conservation in homologues. We thus speculate a possible involvement of these residues in cation binding and/or transport. We do not know at present whether these residues of ShaA assemble in close proximity to each other to form an ion translocation site, or if they function independently.

By performing multiple alignments of other Sha proteins, we observed that Asp-121 in ShaB, Asp-75 and Glu-137 in ShaD (corresponding to Asp-50 and Glu-113 in ShaA, respectively), Glu-67 in ShaE, and Asp-38 in ShaF of *B. subtilis* were also highly conserved and predicted to be embedded in transmembrane segments. We are currently investigating the involvement of these conserved acidic residues in ion transport.

## Acknowledgements

We thank T. Tsuchiya (Okayama University, Japan) for providing *E. coli* KNabc. This work was partially supported by grants for the Bioarchitect Research and Eco-Molecular Research Programs from RIKEN. This work was also supported by a Grant-in-Aid for Scientific Research for Young Scientists (B) from the Ministry of Education, Culture, Sports, Science and Technology of Japan to S. K.

## References

[1] M. Ito, A.A. Guffanti, B. Oudega, T.A. Krulwich, mrp, a multigene, multifunctional locus in *Bacillus subtilis* with roles in resistance to cholate and to $Na^+$ and in pH homeostasis, J. Bacteriol. 181 (1999) 2394–2402.

[2] T. Hiramatsu, K. Kodama, T. Kuroda, T. Mizushima, T. Tsuchiya, A putative multisubunit $Na^+/H^+$ antiporter from *Staphylococcus aureus*, J. Bacteriol. 180 (1998) 6642–6648.

[3] P. Putnoky, A. Kereszt, T. Nakamura, G. Endre, E. Grosskopf, P. Kiss, A. Kondorosi, The pha gene cluster of *Rhizobium meliloti* involved in pH adaptation and symbiosis encodes a novel type of $K^+$ efflux system, Mol. Microbiol. 28 (1998) 1091–1101.

[4] T.H. Swartz, S. Ikewada, O. Ishikawa, M. Ito, T.A. Krulwich, The Mrp system: a giant among monovalent cation/proton antiporters? Extremophiles 9 (2005) 345–354.

[5] T. Hamamoto, M. Hashimoto, M. Hino, M. Kitada, Y. Seto, T. Kudo, K. Horikoshi, Characterization of a gene responsible for the $Na^+/H^+$ antiporter system of alkaliphilic *Bacillus* species strain C-125, Mol. Microbiol. 14 (1994) 939–946.

[6] S. Kosono, S. Morotomi, M. Kitada, T. Kudo, Analyses of a *Bacillus subtilis* homologue of the $Na^+/H^+$ antiporter gene which is important for pH homeostasis of alkaliphilic *Bacillus* sp. C-125, Biochim. Biophys. Acta 1409 (1999) 171–175.

[7] S. Kosono, K. Haga, R. Tomizawa, Y. Kajiyama, K. Hatano, S. Takeda, Y. Wakai, M. Hino, T. Kudo, Characterization of a multigene-encoded sodium/hydrogen antiporter (Sha) from *Pseudomonas aeruginosa*: its involvement in pathogenesis, J. Bacteriol. 187 (2005) 5242–5248.

[8] C. Mathiesen, C. Hägerhäll, The antiporter module of respiratory chain complex I includes the MrpC/NuoK subunit—a revision of the modular evolution scheme, FEBS Lett. 549 (2003) 7–13.

[9] M. Ito, A.A. Guffanti, W. Wang, T.A. Krulwich, Effects of nonpolar mutations in each of the seven *Bacillus subtilis mrp* genes suggest complex interactions among the gene products in support of $Na^+$ and alkali but cholate resistance, J. Bacteriol. 182 (2000) 5663–5670.

[10] T. Yoshinaka, H. Takasu, R. Tomizawa, S. Kosono, T. Kudo, A shaE deletion mutant showed lower $Na^+$ sensitivity compared to other deletion mutants in the *Bacillus subtilis sodium*/hydrogen antiporter (Sha) system, J. Biosci. Bioeng. 95 (2003) 306–309.

[11] T. Friedrich, D. Scheide, The respiratory complex I of bacteria, archaea and eukarya and its module common with membrane-bound multisubunit hydrogenases, FEBS Lett. 479 (2000) 1–5.

[12] J. Steuber, $Na^+$ translocation by bacterial NADH:quinone oxidoreductases: an extension to the complex-I family of primary redox pumps, Biochim. Biophys. Acta 1505 (2001) 45–56.

[13] C. Mathiesen, C. Hägerhäll, Transmembrane topology of the NuoL, M and N subunits of NADH:quinone oxidoreductase and their homologues among membrane-bound hydrogenases and bona fide antiporters, Biochim. Biophys. Acta 1556 (2002) 121–132.

[14] P.J. Silva, E.C.D. van den Ban, H. Wassink, H. Haaker, B. de Castro, F.T. Robb, W.R. Hagen, Enzymes of hydrogen metabolism in *Pyrococcus furiosus*, Eur. J. Biochem. 267 (2000) 6541–6551.

[15] R. Sapra, M.F.J.M. Verhagen, M.W.W. Adams, Purification and characterization of a membrane-bound hydrogenase from the hyperthermophilic archaeon *Pyrococcus furiosus*, J. Bacteriol. 182 (2000) 3423–3428.

[16] R. Sapra, K. Bagramyan, M.W.W. Adams, A simple energy-conserving system: proton reduction coupled to proton translocation, Proc. Natl. Acad. Sci. U. S. A. 100 (2003) 7545–7550.

[17] P. Dibrov, L. Fliegel, Comparative molecular analysis of $Na^+/H^+$ exchangers: a unified model for $Na^+/H^+$ antiport? FEBS Lett. 424 (1998) 1–5.

[18] M. Kervinen, J. Patsi, M. Finel, I.E. Hassinen, A pair of membrane-embedded acidic residues in the NuoK subunit of *Escherichia coli* NDH-1, a counterpart of the ND4L subunit of the mitochondrial complex I, are required for high ubiquinone reductase activity, Biochemistry 43 (2004) 773–781.

[19] M.C. Kao, S. Di Bernardo, M. Perego, E. Nakamaru-Ogiso, A. Matsuno-Yagi, T. Yagi, Functional roles of four conserved charged residues in the membrane domain subunit NuoA of the proton-translocating NADH-quinone oxidoreductase from *Escherichia coli*, J. Biol. Chem. 279 (2004) 32360–32366.

[20] K. Nozaki, K. Inaba, T. Kuroda, M. Tsuda, T. Tsuchiya, Cloning and sequencing of the gene for $Na^+/H^+$ antiporter of *Vibrio parahaemolyticus*, Biochem. Biophys. Res. Commun. 222 (1996) 774–779.

[21] E.B. Goldberg, T. Arbel, J. Chen, R. Karpel, G.A. Mackie, S. Schuldiner, E. Padan, Characterization of a $Na^+/H^+$ antiporter gene of *Escherichia coli*, Proc. Natl. Acad. Sci. U. S. A. 84 (1987) 2615–2619.

[22] J.D. Thompson, T.J. Gibson, F. Plewniak, F. Jeanmougin, D.G. Higgins, The CLUSTAL_X windows interface: flexible strategies for multiple sequence alignment aided by quality analysis tools, Nucleic Acids Res. 25 (1997) 4876–4882.

[23] T. Hirokawa, S. Boon-Chieng, S. Mitaku, SOSUI: classification and secondary structure prediction system for membrane proteins, Bioinformatics 14 (1998) 378–379.

[24] E.L. Sonnhammer, G. von Heijne, A. Krogh, A hidden Markov model for predicting transmembrane helices in protein sequences, Proc. Int. Conf. Intell. Syst. Mol. Biol. 6 (1998) 175–182.

[25] G.E. Tusnady, I. Simon, Principles governing amino acid composition of integral membrane proteins: application to topology prediction, J. Mol. Biol. 283 (1998) 489–506.

[26] K. Hofmann, W. Stoffel, TMbase — a database of membrane spanning proteins segments, Biol. Chem. Hoppe-Seyler 374 (1993) 166.

[27] B. Rost, R. Casadio, P. Fariselli, C. Sander, Transmembrane helices predicted at 95% accuracy, Protein Sci. 4 (1995) 521–533.

[28] M. Cserzo, E. Wallin, I. Simon, G. von Heijne, A. Elofsson, Prediction of transmembrane alpha-helices in procariotic membrane proteins: the Dense Alignment Surface method, Protein Eng. 10 (1997) 673–676.

[29] N. Fisher, P.R. Rich, A motif for quinone binding sites in respiratory and photosynthetic systems, J. Mol. Biol. 296 (2000) 1153–1162.

[30] E. Nakamaru-Ogiso, K. Sakamoto, A. Matsuno-Yagi, H. Miyoshi, T. Yagi, The ND5 subunit was labeled by a photoaffinity analogue of fenpyroximate in bovine mitochondrial Complex I, Biochemistry 42 (2003) 746–754.

[31] M. Ito, A.A. Guffanti, T.A. Krulwich, Mrp-dependent $Na^+/H^+$ antiporters of Bacillus exhibit characteristics that are unanticipated for completely secondary active transporters, FEBS Lett. 496 (2001) 117–120.

[32] E. Padan, T. Tzubery, K. Herz, L. Kozachkov, A. Rimon, L. Galili, NhaA of *Escherichia coli*, as a model of a pH-regulated $Na^+/H^+$ antiporter, Biochim. Biophys. Acta 1658 (2004) 2–13.

[33] J. Steuber, The C-terminally truncared NuoL subunit (ND5 homologue) of the $Na^+$-dependent complexI from *Escherichia coli* transports $Na^+$, J. Biol. Chem. 278 (2003) 26817–26822.

[34] L. Galili, K. Herz, O. Dym, E. Padan, Unraveling functional and structural interactions between transmembrane domains IV and XI of NhaA $Na^+/H^+$ antiporter of *Escherichia coli*, J. Biol. Chem. 279 (2004) 23104–23113.

[35] T.H. Swartz, M. Ito, D.B. Hicks, M. Nuqui, A.A. Guffanti, T.A. Krulwich, The Mrp $Na^+/H^+$ antiporter increases the activity of the malate:quinone oxidoreductase of an *Escherichia coli* respiratory mutant, J. Bacteriol. 187 (2005) 388–391.

[36] H. Inoue, T. Noumi, T. Tsuchiya, H. Kanazawa, Essential aspartic acid residues, Asp-133, Asp-163 and Asp-164, in the transmembrane helices of a $Na^+/H^+$ antiporter (NhaA) from *Escherichia coli*, FEBS Lett. 363 (1995) 264–268.

[37] C. Hunte, E. Screpanti, M. Venturi, A. Rimon, E. Padan, H. Michel, Structure of a $Na^+/H^+$ antiporter and insights into mechanism of action and regulation by pH, Nature 435 (2005) 1197–1202.